Thermal transformation of quaternary compounds in NaF–CaF$_2$–AlF$_3$ system

Julia N. Zaitseva [a], Igor S. Yakimov [b], Sergei D. Kirik [a,b,*]

[a] *Institute of Chemistry and Chemical Technology SB RAS, K. Marx St., 42, Krasnoyarsk 660049, Russia*
[b] *Siberian Federal University, Svobodny Str., 79, Krasnoyarsk 660041, Russia*

ARTICLE INFO

ABSTRACT

Details of quaternary compounds formation in the system NaF–CaF$_2$–AlF$_3$ are specified. To achieve this aim, the samples of phases NaCaAlF$_6$ and Na$_2$Ca$_3$Al$_2$F$_{14}$ have been obtained by high-temperature solid-phase synthesis. Their thermal behavior when heated up to 800 °C has been studied using the methods of high-temperature X-ray diffraction (XRD) and thermal analysis (TA). The system under consideration can be regarded as a quasibinary section CaF$_2$–NaAlF$_4$, where at $T = 745$–750 °C invariant equilibrium is implemented with the phases CaF$_2$–NaCaAlF$_6$–Na$_2$Ca$_3$Al$_2$F$_{14}$–(liquid melt)–(NaAlF$_4$). The peculiarity of the equilibrium is NaAlF$_4$ metastability at normal pressure. Below the equilibrium temperature the quaternary phase Na$_2$Ca$_3$Al$_2$F$_{14}$ is stable and NaCaAlF$_6$ above this temperature. The phase NaCaAlF$_6$ fixed by rapid quenching from high temperatures and when heated up to 640 °C decomposes, yielding Na$_2$Ca$_3$Al$_2$F$_{14}$. Further heating in vacuum at temperature up to 740 °C results in decomposition of Na$_2$Ca$_3$Al$_2$F$_{14}$ into CaF$_2$ and Na$_3$AlF$_6$. The expected reverse transformation of Na$_2$Ca$_3$Al$_2$F$_{14}$ into NaCaAlF$_6$ has not been observed under experimental conditions. Transformations in bulk samples reveal direct and reverse transformation of quaternary phases.

Synopsis: Thermal transformation of the quaternary compounds in system (NaF–CaF$_2$–AlF$_3$) was investigated using high-temperature X-ray diffraction (XRD) and thermal analysis (TA). In the system the invariant equilibrium is implemented with the phases CaF$_2$–NaCaAlF$_6$–Na$_2$Ca$_3$Al$_2$F$_{14}$–(liquid melt)–(NaAlF$_4$) at $T = 745$–750 °C.

1. Introduction

The significance of the quasiternary system Na$_3$AlF$_6$–AlF$_3$–CaF$_2$ diagram could hardly be overestimated for the aluminum production [1,2]. It was repeatedly investigated in 20th century. However, there are still blank spots which induce some problems with the electrolysis control. Because of the high volatility of electrolyte components at the electrolysis temperature operation there is a necessity to correct the electrolyte composition from time to time [3–5]. The correction is carried out after an electrolyte analysis. The electrolyte composition is defined by X-ray diffraction (XRD) using crystallized samples. Their composition is presented by a number of crystal phases: Na$_3$AlF$_6$ (cryolite), Na$_5$Al$_3$F$_{14}$ (chiolite), CaF$_2$ (fluorite) and others. The procedure of quantitative XRD provides the concentration of each present phase converted into the concentration of chemical components. Particularly, the content of CaF$_2$ is determined, and the key technological parameter—cryolite ratio (CR)—is calculated: CR = NaF (mol)/AlF$_3$ (mol)—molar ratio of sodium fluoride to aluminum fluoride, or in another term—excess of AlF$_3$ concentration [1]. The quantitative phase determination by XRD in electrolytes containing calcium presents methodical problem. In the course of crystallization calcium fluoride forms three phases: CaF$_2$ (fluorite), NaCaAlF$_6$ and Na$_2$Ca$_3$Al$_2$F$_{14}$ (calcium cryolites). The measurement of NaCaAlF$_6$ meets a problem because of its poor crystallinity. It has been mentioned in literature that the correlation between calcium phases changes depending both on electrolyte composition and sampling procedure [3,6,7]. Unfortunately, the equilibrium system of calcium-containing phases is still unclear, which does not allow one to substantiate adequate electrolyte sampling procedure providing samples of a required quality.

Phase diagrams of cryolite-containing systems [1] have mainly been studied focusing at the "liquidus" part for determining the temperatures of the melt crystallization. However, for the purposes of electrolyte composition control by XRD subsolidus part appears to have great importance. The available information about this temperature range of the system is fragmentary and contradictory [1,8,9]. The ternary system Na$_3$AlF$_6$–AlF$_3$–CaF$_2$ which is a part of more general system NaF–AlF$_3$–CaF$_2$ was investigated during the 20th century. As early as in 1912, Fedotiev and Ilinskii [10], using the data of crystal-optical analysis, made the first description of the system, having found crystalline

phases: NaF, Na_3AlF_6, $Na_5Al_3F_{14}$, AlF_3, CaF_2. Pfundt and Zimmermann [11] established one more compound existing in this system—$NaCaAlF_6$—which melts incongruently. A diagram fragment limited to the compounds Na_3AlF_6–AlF_3–CaF_2 was reported by Craig and Brawn [8] in 1980. The work revealed the existence of two compounds with the following composition: $NaCaAl_2F_9$ and $NaCaAlF_6$. As a whole, the following phases can crystallize in the system: CaF_2, Na_3AlF_6, $Na_5Al_3F_{14}$, Ca_2AlF_7, $CaAlF_5$, AlF_3, $NaCaAlF_6$, $NaCaAl_2F_9$. Later, in 1985, Baggio [12] made a correction and found out that the real composition of the phase $NaCaAl_2F_9$ corresponds to the compound $Na_2Ca_3Al_2F_{14}$. Soon after it was confirmed by crystal structure investigations [13–15]. Anufrieva et al. [9] in 1985, reported a diagram of the system NaF–AlF_3–CaF_2, according to which seven chemical compounds are formed including three congruently melting compounds: Na_3AlF_6, $NaAlF_4$, $CaAlF_5$, and four incongruently melting ones: $Na_5Al_3F_{14}$, $NaCaAlF_6$, $NaCaAl_2F_9$, Ca_2AlF_7.

On the basis of the differential thermal analysis (TA) data for the system Na_3AlF_6–$NaCaAlF_6$ Craig and Brawn [8] found that $NaCaAlF_6$ existed in three polymorphous modifications with the transition temperatures 610 and 722 °C. The phase $NaCaAlF_6$ is retained at 600 °C for 20 h; however, with increasing the time of annealing up to 100 h, $NaCaAlF_6$ is converted into $NaCaAl_2F_9$ (as mentioned above, the correct composition $Na_2Ca_3Al_2F_{14}$). Wide ranges of solid solutions were not found in the system [16].

On the whole, the data available in literature describe the crystallization of phases in the system. However, the phase composition of industrial electrolytes is more diversified than that expected according to the phase equilibrium diagram. It has to be noted that the revealed crystallization areas of the compounds $NaCaAlF_6$, $Na_2Ca_3Al_2F_{14}$, Ca_2AlF_7 and $CaAlF_5$, as well as eutectic and peritectic points given in the above mentioned works [8,9], do not coincide in many cases. The most substantial is the fact that the data available are not sufficient to explain phase formation mechanism observed when sampling in industry and to formulate sound recommendations for sampling.

In the present paper details of the quaternary phase crystallization in the system NaF–CaF_2–AlF_3 are specified. The individual phases $NaCaAlF_6$, $Na_2Ca_3Al_2F_{14}$ were synthesized and high-temperature XRD and thermal studies of their transformations were carried out at heating. When cooled the behavior of these phases in the electrolyte composition depending on the cooling rate and electrolyte composition (CR) has been studied. The effect of temperature annealing in the subsolidus area on decomposition and formation of calcium-containing phases in electrolytes has been investigated as well.

2. Experimental

2.1. Synthesis of $NaCaAlF_6$ and $Na_2Ca_3Al_2F_{14}$

Crystal phases $NaCaAlF_6$ and $Na_2Ca_3Al_2F_{14}$ were synthesized from stoichiometric mixtures of individual fluorides AlF_3, NaF and CaF_2 by high-temperature solid-phase synthesis. Temperature regimes were chosen with respect to recommendations [12]. The carefully blended mixture of fine powders of initial components of 10 g mass was loaded into platinum crucible with a head and was placed in a heated furnace at $T = 740$ °C for an hour. Then, in case of $NaCaAlF_6$ the crucible was taken out of the furnace and air-cooled. The mass loss when synthesizing was about 1.2 mass%. In case of $Na_2Ca_3Al_2F_{14}$ after keeping in furnace for an hour at 740 °C, the temperature was reduced to 565 °C and kept for 20 h. The mass loss was about 1.4%. The substances obtained were analyzed by XRD. XRD patterns are given in Fig. 1a, b.

XRD data are in agreement with XRD reference data ICDD-JCPDS-PDF-2 [17,18]. The phases $Na_5Al_3F_{14}$, CaF_2 for $Na_2Ca_3Al_2F_{14}$ have been recorded as admixtures.

2.2. Synthesis of calcium-containing electrolytes

To study the behavior of the calcium-containing phases in electrolyte medium the electrolytes E1, E2, E3 with CR 1.9, 2.4, 2.7, respectively, and the same CaF_2 concentration equal to 8 mass% were synthesized from the correspondent mixtures of the fluorides AlF_3, NaF, and CaF_2. The mixtures of the initial fluorides with the mass of 10 g were melted in a closed platinum crucible in a furnace at the temperature range from 960 to 1000 °C (depending on the CR value), for 20 min. Later, three different ways of cooling were used: (1) the sample was cast into a massive metallic mold at 25 °C, (2) the sample was taken out of the furnace and air-cooled; (3) the sample was cooled in the furnace at a rate of 8 °C/min up to one of the fixed temperatures of 560, 610 and 710 °C; then, the electrolyte was kept at these temperatures for 30 min, and air-cooled.

2.3. TA

TA of the samples of the $NaCaAlF_6$ and $Na_2Ca_3Al_2F_{14}$ phases was carried out using a MOM Q-1000 Derivatogragh in platinum crucibles with a head and a weight of 500 mg, in the temperature range from 25 to 860 °C in air with a heating rate of 10 °C/min. Thermograms are given in Fig. 2.
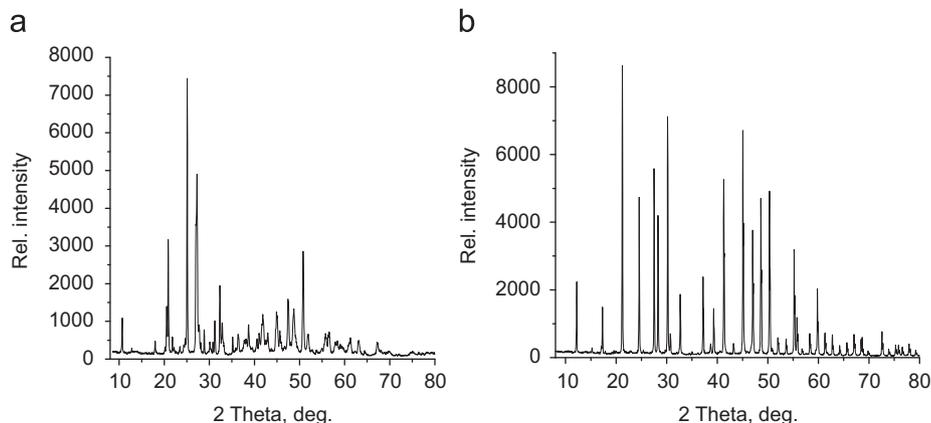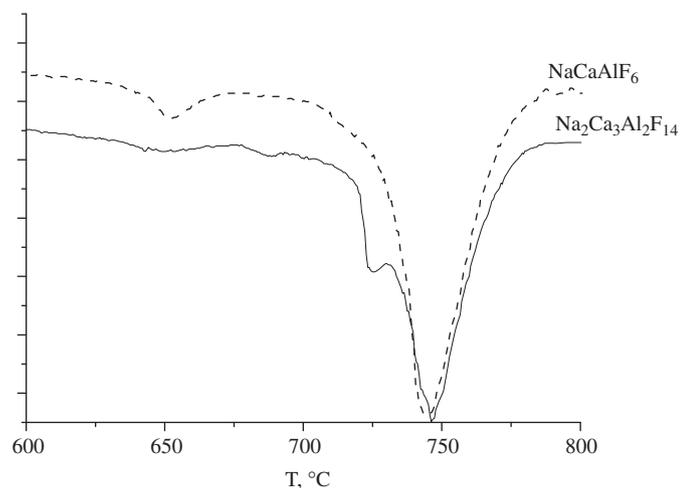

Fig. 1. (a) X-ray diffraction patterns of $NaCaAlF_6$ [18]; (b) X-ray diffraction patterns of $Na_2Ca_3Al_2F_{14}$ [17].

Fig. 2. Thermograms for phases $NaCaAlF_6$ and $Na_2Ca_3Al_2F_{14}$ at heating. The peak at 655 °C corresponds to transformation of $NaCaAlF_6$ into $Na_2Ca_3Al_2F_{14}$, the peak at $T = 695$ °C corresponds to eutectics $Na_5Al_3F_{14}$–$NaAlF_4$, the peak at 725–735 °C corresponds to peritectic $Na_5Al_3F_{14}$–Na_3AlF_6, the peak at 745–750 °C corresponds to decomposition of $Na_2Ca_3Al_2F_{14}$ into CaF_2 and Na_3AlF_6.

2.4. XRD analysis

XRD patterns were taken using X'Pert Pro (PANalitical) diffractometer, equipped with PIXel detector with a graphite monochromator using $CuK\alpha$ radiation, in the range from 10° to 80° with a step of 0.026° (2Θ), the total scanning time being 12 min. The sample was prepared by a method of direct loading in a sample holder with a diameter of 27 mm.

High-temperature XRD investigations were carried out using X'Pert Pro (PANalitical) diffractometer with a high temperature chamber NTK1200N "Anton Paar" in vacuum. The sample with mass of 200 mg was prepared in a flat alumina sample holder with a diameter of 10 mm. The temperature was increased at a rate of 50 °C/min to certain value and then, for 5 min XRD patterns were taken in the range from 5° to 80° (2Θ). Then, the process was repeated at the next temperature stage.

3. Results and discussion

Fig. 3 presents a composition triangle of the system NaF–CaF_2–AlF_3 with the area of the "working electrolytes" being marked, where the investigations were carried out; also marked are the positions of the main calcium-containing phases occurring in the cooled electrolyte samples. The presence of four and sometimes five phases in the electrolyte samples contradicts Gibbs's phase rule and indicates non-equilibrium conditions of their obtaining. The system peculiarity is the location of the ternary phases on the section of CaF_2–$NaAlF_4$. This allows one to confine the possible electrolyte composition field by the triangle CaF_2–Na_3AlF_6–$NaAlF_4$. The double fluoride phases Ca_2AlF_7 and $CaAlF_5$ have never occurred in the electrolyte samples and it is a well-grounded argument for marking this triangle field.

High-temperature XRD of the phases $NaCaAlF_6$ and $Na_2Ca_3Al_2F_{14}$ were carried out by multistage heating in vacuum. The $NaCaAlF_6$ sample was heated with intermediate data obtained at 100, 300, 400, 500, 550, 570, 600 °C. Some of the XRD patterns are given in Fig. 4. More detailed information is presented in [19]. Below 400 °C the phase $NaCaAlF_6$ undergoes structural transformation retaining its composition. At 500 °C (Fig. 4) the process of $NaCaAlF_6$ decomposition with the formation of
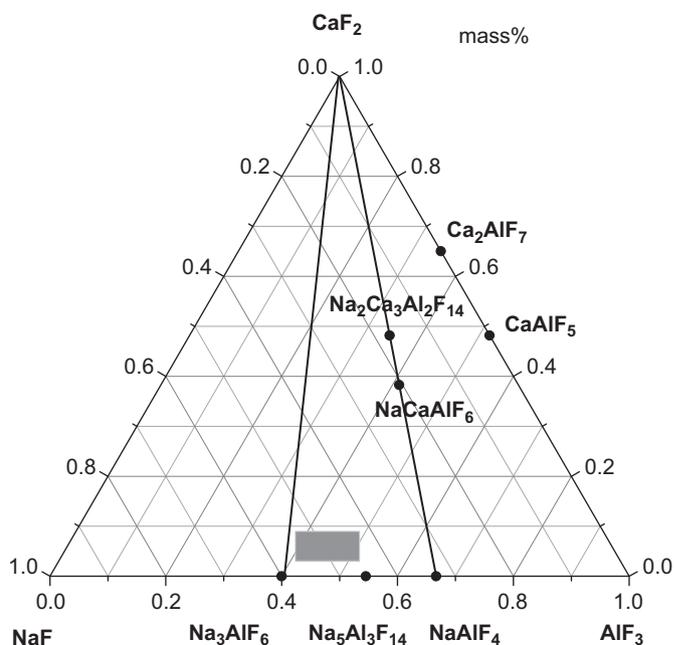
Fig. 3. Composition triangle of the system NaF–CaF_2–AlF_3. The positions of the main phases occurring in the electrolyte are marked. The field of the "industrial electrolyte" composition is marked by the color spot.
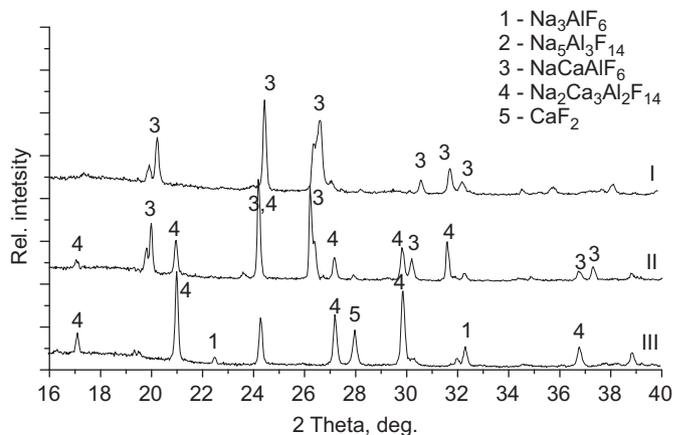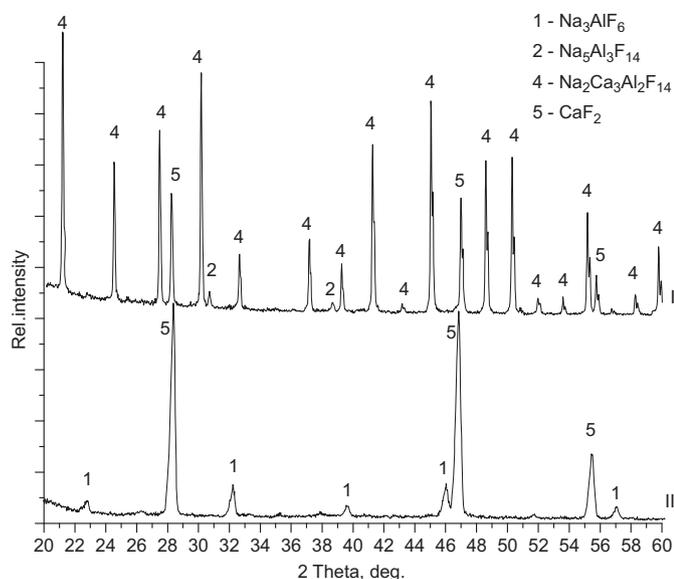

Fig. 4. X-ray diffraction patterns of the sample of $NaCaAlF_6$ taken in X-ray high-temperature chamber I—at 25 °C, II—at 500 °C, III—at 500 °C, 1 h. At 500 °C structural changes of the phase $NaCaAlF_6$ are observed; the lines of the phase $Na_2Ca_3Al_2F_{14}$ appear (middle pattern). After exposure during 1 h to 500 °C, the phase $NaCaAlF_6$ disappears; the content of $Na_2Ca_3Al_2F_{14}$, CaF_2 and Na_3AlF_6 increases.

$Na_2Ca_3Al_2F_{14}$ begins in accordance with the equation

$$3NaCaAlF_6 \rightarrow Na_2Ca_3Al_2F_{14} + NaAlF_4$$

Among the reaction products the phase $NaAlF_4$ was not observed; that is likely to be explained by its high instability. In vacuum at 500 °C the complete transformation of $NaCaAlF_6$ into $Na_2Ca_3Al_2F_{14}$ was observed after 1 h as well as the beginning of $Na_2Ca_3Al_2F_{14}$ decomposition with the formation of Na_3AlF_6 and CaF_2.

Heating $Na_2Ca_3Al_2F_{14}$ in high-temperature XRD chamber has shown that the phase remains approximately up to 600 °C and then, decomposition begins. Only two decomposition products, CaF_2 and Na_3AlF_6, are shown in the X-ray patterns (Fig. 5), which cannot explain the mass balance without assuming volatile phase

Fig. 5. X-ray diffraction patterns of the sample $Na_2Ca_3Al_2F_{14}$ taken in X-ray high-temperature chamber I—at 25 °C, II—at 600 °C. The phase $Na_2Ca_3Al_2F_{14}$ disappears, the phases CaF_2 and Na_3AlF_6 are observed.

contribution. Assuming that the decomposition occurs within the framework of the quasibinary system CaF_2–$NaAlF_4$, the observed process can be described by the equation system

$$Na_2Ca_3Al_2F_{14} \rightarrow 2NaAlF_4 + 3CaF_2$$

$$3NaAlF_4 \rightarrow Na_3AlF_6 + 2AlF_3$$
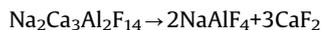
The presence of Na_3AlF_6 in the products indicates the fact that the $NaAlF_4$ stability at low pressure is limited and its decomposition takes place directly in the sample. No solid-phase decomposition reaction of $Na_2Ca_3Al_2F_{14}$ into $NaCaAlF_6$ and CaF_2 is observed.

The final products belong to a quasibinary system of eutectic type, CaF_2–Na_3AlF_6, with the melting point of the eutectic being 945 °C [16]. When cooled the phase transformation β-$Na_3AlF_6 \rightarrow \alpha$-$Na_3AlF_6$ occurs in the system.

The existence of the phase $NaAlF_4$ has been repeatedly mentioned in literature [1,9,20–24] but reliable information is absent. The phase $NaAlF_4$, according to [20], is formed by peritectic reaction at 710 °C and decomposes already at 680 °C:

$$NaAlF_4(s) \rightarrow 1/5\ Na_5Al_3F_{14}(s) + 2/5\ AlF_3(s)$$

Holm et al. [21] published X-ray diffraction data for $NaAlF_4$, which were repeated in some papers [22,23]. The structure of compound is not known. At the present study the phase $NaAlF_4$ was not observed among the solid products of decomposition in the sample; however, the traces of the substance were detected in the products condensed in cooled parts of the X-ray high-temperature chamber.

This is likely to cause the necessity of creating special conditions for maintaining appropriate vapor pressure above the substances in order to fix highly volatile and unstable components. Due to the technical limitations, as contrasted to the requirements given in this work, the transformations were carried out either in vacuum or in the air, with the sample mass being comparatively small. These conditions hindered $NaAlF_4$ observations in the sample. The formed phase $NaAlF_4$ could evaporate

away from the reaction zone, decompose or react with other medium components, according to the equations

$$3NaAlF_4 \rightarrow Na_3AlF_6 + 2AlF_3$$

$$2NaAlF_4 + Na_3AlF_6 \rightarrow Na_5Al_3F_{14}$$

The conducted high-temperature experiments have demonstrated that calcium-containing phases have different temperature intervals of stability. The phase $NaCaAlF_6$ is metastable at low temperatures. Its relaxation in the conditions of low pressures begins at 500 °C and reveals the transformation into $Na_2Ca_3Al_2F_{14}$. No reverse transformation is observed in the experiment conditions.

It is obvious that the results obtained only partially reflect the processes occurring when cooling the electrolyte samples. For this reason an additional number of experiments were carried out connected with electrolyte sample cooling from the melt condition at different rates, including exposure to different temperatures during the process of cooling.

XRD analysis of the products has shown that no changes of the phase composition occur when changing crystallization rate. The following phases are observed: Na_3AlF_6, $Na_5Al_3F_{14}$, $NaCaAlF_6$, $Na_2Ca_3Al_2F_{14}$ and CaF_2. Faster cooling gives bigger amount of $NaCaAlF_6$. The cooling rate influences the microstructure of particular phases. Specifically, with the increase of the cooling rate the cryolite lines are broadened by 10%. The microstructure of other phases changes very little. Calcium was present in three phases: $NaCaAlF_6$, $Na_2Ca_3Al_2F_{14}$ and CaF_2, with the first phase dominating in the sample with the cryolite ratio 2.7 and the second one in the sample with the cryolite ratio 2.3 and 1.9.

Furnace cooling, including annealing at one of the following temperatures: 740, 610, 560 °C, gives different results. For example, annealing at 740 °C gives rise mainly to $NaCaAlF_6$ crystallization, irrespectively of the cryolite ratio. Annealing at 610 and 560 °C leads to the presence of mainly $Na_2Ca_3Al_2F_{14}$ in the sample.

Based on the results of the experiments carried out the following conclusions can be made. The calcium cryolites formed in the system (NaF–CaF_2–AlF_3) occupy various temperature ranges in the framework of the equilibrium diagram. $Na_2Ca_3Al_2F_{14}$ is a low temperature phase; $NaCaAlF_6$ is a high temperature one. In the cooled electrolyte samples the presence of the two indicated phases simultaneously is a consequence of the non-equilibrium cooling process at which $NaCaAlF_6$ is not completely transformed into $Na_2Ca_3Al_2F_{14}$ and at low temperatures remains in the metastable condition. This circumstance explains the crystal structure degradation and "diffusion" peaks on the diffraction pattern of this phase. It was experimentally proved that dominating crystallization of $Na_2Ca_3Al_2F_{14}$ in industrial samples of electrolytes with low CR is caused by the shift in the composition of the system liquid component at cooling into the concentration field confined with the temperature below 734 °C (incongruent melting of $Na_5Al_3F_{14}$) and above 695 °C (solidus of the subsystem $Na_5Al_3F_{14}$–AlF_3) [1], in which crystallization of $Na_2Ca_3Al_2F_{14}$ occurs.

Transformation of $NaCaAlF_6$ into $Na_2Ca_3Al_2F_{14}$ at cooling occurs during the reaction of decomposition, probably yielding $NaAlF_4$. When heated the reverse reaction does not take place since unstable $NaAlF_4$ is absent in the sample. Instead, the decomposition reaction of the phase $Na_2Ca_3Al_2F_{14}$ on CaF_2 and $NaAlF_4$ is observed with $NaAlF_4$ finally decomposing into cryolite.

Thermograms of the phase heating of $NaCaAlF_6$ and $Na_2Ca_3Al_2F_{14}$ (Fig. 2) can be fully interpreted from the point of view of the processes described. For $NaCaAlF_6$ at 655 °C the process of

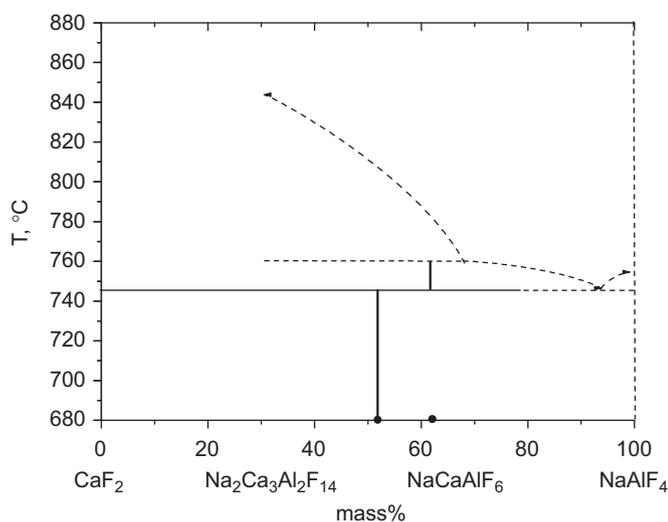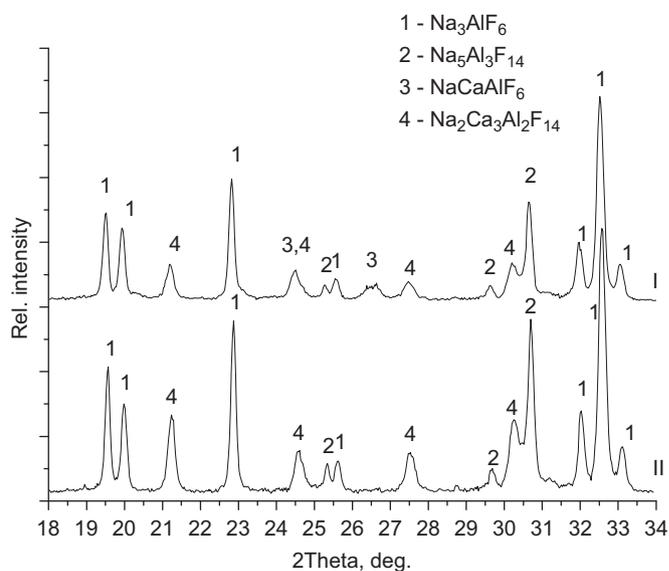**Fig. 6.** The prospective equilibrium diagram of the quasibinary system CaF_2–$NaAlF_4$.

Fig. 7. X-ray diffraction patterns of the industrial electrolyte CR 2.33, $CaF_2 = 7.9$ mass%; I—initial electrolyte the basic phases are Na_3AlF_6 and $Na_5Al_3F_{14}$, calcium is distributed on two phases—$NaCaAlF_6$, $Na_2Ca_3Al_2F_{14}$; II—the sample calcinated at 640 °C 10 min, losses of weight 0.1 mass%; The basic phases—Na_3AlF_6 and $Na_5Al_3F_{14}$, calcium is in one phase—$Na_2Ca_3Al_2F_{14}$.

transformation into the phase $Na_2Ca_3Al_2F_{14}$ is observed. At 745 °C this phase is decomposed into Na_3AlF_6 and CaF_2. On the sample heating curve of the phase $Na_2Ca_3Al_2F_{14}$ there is a number of small peculiarities under 655 °C caused by the admixtures. The temperature of 695 °C corresponds to the eutectic transformation, $Na_5Al_3F_{14}$–AlF_3, and the temperature of 735 °C to the peritectic one, Na_3AlF_6–$Na_5Al_3F_{14}$. The decomposition of $Na_2Ca_3Al_2F_{14}$ occurs at 745 °C.

The transformations considered can be described in the context of the quasibinary system CaF_2–$NaAlF_4$ with invariant five phase equilibrium of CaF_2–$NaCaAlF_6$–$Na_2Ca_3Al_2F_{14}$–(liquid melt)–($NaAlF_4$) at 745 °C. The subsolidus part is given in Fig. 6. The peculiarity of the system is the presence of an unstable and volatile compound, namely of $NaAlF_4$ in the right part of the system. Decomposition of the phase $NaAlF_4$, for example, into $Na_5Al_3F_{14}$ and AlF_3 or Na_3AlF_6 and AlF_3, makes the system split into two subsystems with different equilibrium pressures. It solves the problem of the contradiction to Gibbs's phase rule, which appears since the number of the present phases (five) exceeds the permissible number of phases (four) which are in the equilibrium in the three component system at constant pressure. This gives the basis for the interpretation of the transformations observed. In particular, to approach the equilibrium from below, no formation of $NaCaAlF_6$ occurs, if any external pressure is not applied to the system. In the course of the high-temperature X-ray investigations, which allow the fixation of the solid-phase system components; this condition was not created for technical reasons. Nevertheless, experiments on heating and cooling the bulk sample exhibit the possible presence of both calcium-containing phases simultaneously. Behavior of calcium-containing phases in the samples of industrial electrolyte is illustrated in Fig. 7. The X-ray pattern of the initial electrolyte (Fig. 7, top) shows two phases $NaCaAlF_6$ and $Na_2Ca_3Al_2F_{14}$ containing calcium. After calcinations at 640 °C for 10 min the same sample has lost 0.1 mass% and calcium has been presented in $Na_2Ca_3Al_2F_{14}$.

Thus, quaternary compounds in the system NaF–CaF_2–AlF_3 are presented in phases $NaCaAlF_6$ and $Na_2Ca_3Al_2F_{14}$. They are a part of quasibinary section CaF_2–$NaAlF_4$. In the system at $T = 745$–750 °C the invariant equilibrium is implemented with the phases CaF_2–$NaCaAlF_6$–$Na_2Ca_3Al_2F_{14}$–(liquid melt)–($NaAlF_4$). The quaternary phase $Na_2Ca_3Al_2F_{14}$ is stable below the equilibrium temperature, and $NaCaAlF_6$ above this temperature. The phase $NaCaAlF_6$ can be fixed in metastable state by rapid quenching; however, when

heated up to 640 °C decomposes, yielding $Na_2Ca_3Al_2F_{14}$. The expected reverse transformation of $Na_2Ca_3Al_2F_{14}$ into $NaCaAlF_6$ has not been observed under experimental conditions by high-temperature XRD method. Heating and quenching bulk samples reveal direct and reverse transformation of quaternary phases. The transformations studied allow us to recommend a heat regime strategy for cooling electrolyte samples which are selected for the composition monitoring. Cooling with the short-time delay (annealing) in the temperature range of 560–640 °C, in which the full transformation of the phase $NaCaAlF_6$ into $Na_2Ca_3Al_2F_{14}$ occurs, permits obtaining industrial electrolyte samples which would be more suitable for the measurement by the XRD method and application of full profile refinement as data processing methods [25,26].

References

[1] K. Grjotheim, C. Krohn, M. Malinovsky, K. Matiasovsky, Aluminium Electrolysis, Fundamentals of the Hall–Heroult Process, second ed., Aluminum-Verlag, Dusseldorf, 1982.
[2] J. Thonstad, S. Rolseth, Travaux du Comite International pour l'Etude des Bauxites, de l'Alumine et de l'Aluminium 30 (2003) 134–140.
[3] S.D. Kirik, N.N. Kulikova, I.S. Yakimov, T.I. Klueva, I.A. Baranov, V.Yu. Buzunov, V.G. Goloschapov, Nonferrous Met. 9 (1996) 75–77.
[4] S.D. Kirik, I.S. Yakimov, N.N. Golovnev, J.N. Zaitseva, S.G. Ruzhnikov, A.M. Sayutin, in: The International Conference—Aluminium of Siberia 2002, Krasnoyarsk, 2002, pp. 400–404.
[5] Combined XRD/XRF System for Potflux Analysis PW1760/10. Instructional Manual 9499-303-01711, 840127 Almelo, The Netherlands.
[6] L.P. Lossius, H. Hoie, H.H. Pedersen, T. Foosnaes, Light Metals (2000) 265–270.
[7] S.D. Kirik, I.S. Yakimov, S.G. Ruzhnikov, in: The International Conference—Aluminium of Siberia 2001, Krasnoyarsk, 2001, pp. 213–219.
[8] D.F. Craig, J. Brawn Jr., Am. Ceram. Soc. 63 (1980) 254–261.
[9] N.I. Anufrieva, Z.N. Balashova, V.N. Veretinskiy, Nonferrous Met. 8 (1985) 66–71.
[10] P.P. Fedotiev, V.P. Ilinskii, Z. Anorg. Allg.Chem. 129 (1923) 93–107.
[11] H. Pfundt, N. Zimmermann, Erzmetall. Bd. 25 (11) (1972) 564–567.
[12] S. Baggio, G. Massiff, J. Appl. Crystallogr. (1985) 537–539.
[13] A. Hemon, G. Courbion, J. Solid State Chem. 84 (1990) 153–164.
[14] G. Courbion, G. Ferey, J. Solid State Chem. 76 (1988) 426–431.
[15] A. Le Bail, A. Hemond Ribaud, G. Courbion, Eur. J. Solid State Inorg. Chem. 35 (1998) 265–272.
[16] J.L. Holm, Acta Chem. Scand. 22 (1968) 1004–1012.
[17] ICDD-JCPDS PDF2 file, # 01-084-1651, Pennsylvania, USA.
[18] ICDD-JCPDS PDF2 file, # 00-046-0600, Pennsylvania, USA.

[19] J.N. Zaitseva, E.N. Lyndina, I.S. Yakimov, S.D. Kirik, J. Sib. Fed. Univ. Chem. 1 (3) (2008) 260–268.
[20] H. Ginsberg, K. Wefers, Z. Erzbergbau Metallhuettenwes. 20 (4) (1967) 156–161.
[21] M. Bruno, O. Herstad, J.L. Holm, Acta Chem. Scand. 52 (1998) 1399–1401.
[22] O. Bj½rseth, O. Herstad, J.L. Holm, Acta Chem. Scand. A 40 (1986) 566–571.
[23] Z. Qiu, J. Zhang, K. Grotheim, H. Kvand, Light Met. (1991) 315–320.
[24] N.V. Golovnykh, A.A. Tupitsyn, V.A. Bychinskii, A.S. Zolotova, Izv. Vyssh. Uchebn. Zaved. Tsvetn. Metall. 5 (2008) 33–37.
[25] K. Knorr, Publ. Aust. Inst. Min. Metall. 8 (2008) 125–131.
[26] K. Knorr, C. Kelaart, Miner. Eng. 22 (2009) 434–439.